

## All-optical control and direct detection of ultrafast spin polarization in a multi-valence-electron system

Takashi Nakajima,<sup>1,2,\*</sup> Yukari Matsuo,<sup>2</sup> and Tohru Kobayashi<sup>2</sup>

<sup>1</sup>*Institute of Advanced Energy, Kyoto University, Gokasho, Uji, Kyoto 611-0011, Japan*

<sup>2</sup>*RIKEN (The Institute of Physical and Chemical Research), 2-1 Hirosawa, Wako, Saitama 351-0198, Japan*

(Received 24 July 2007; published 3 June 2008)

We demonstrate all-optical control of ultrafast spin polarization upon breakup of a multi-valence-electron system using two-color pump-probe photoionization. For the direct detection of spin polarization, we measure the laser-induced fluorescence of photoions. The experimental results agree well with our *ab initio* theory.

DOI: [10.1103/PhysRevA.77.063404](https://doi.org/10.1103/PhysRevA.77.063404)

PACS number(s): 32.80.Rm, 32.80.Qk, 42.50.Md, 42.65.Re

Investigation of the control of atoms and molecules using lasers [1,2] has attracted much attention in recent years. Its goal is to control the external as well as internal degrees of freedom in a system. The ideas and the techniques developed in atomic and molecular physics for coherent control are quite versatile. Indeed, many ideas and techniques developed in atomic and molecular physics have been exported to other branches of physics and chemistry.

For *ultrafast* coherent control, a pair of time-delayed pulses is often used to induce quantum mechanical interference [3] in one way or another. By changing the time delay between the two pulses, constructive or destructive interference is induced in a system. For the purpose of ultrafast coherent control, the pulse does not always have to be transform limited. As a matter of fact, frequency-chirped optical pulses can be conveniently used for some specific cases [4,5].

So far most of the studies in coherent control in atomic and molecular physics have focused on the *selectivity* of a specific state (target state) without controlling the *spin degree of freedom*. Closely related to this, a pump-probe scheme has been applied to atoms of the alkali metal K, to create a coherent superposition of fine structure doublets of  $4p_{1/2}$  and  $4p_{3/2}$ , and a quantum beat was experimentally observed in the  $K^+$  ion signal [6]. The use of fine structure doublets and equivalently spin-orbit interactions led to the idea of polarizing photoelectrons with circularly polarized pulses [6], which was theoretically studied in more detail in the authors' later paper [7]. These experiments [6], however, do not reveal any evidence of spin polarization, since it was  $K^+$  ions that were detected. Note that the alkali-metal ion cannot be spin polarized, since it has a closed-shell structure. Moreover, linear polarization was employed for both pump and probe pulses. It is clear that the use of a circularly polarized pulse and spin-resolved detection of photoelectrons would be necessary to detect ultrafast spin polarization with alkali-metal atoms.

In contrast, the use of alkaline-earth-metal atoms has a certain advantage in terms of producing and observing spin-polarized species. One of the main advantages of using alkaline-earth-metal atoms over alkali-metal atoms is that both photoions and photoelectrons can potentially be polar-

ized if an appropriate scheme is chosen [8]. Moreover, detection of the spin of photoions can be optically performed [9,10], although detection of the spin of photoelectrons still requires the use of a Mott-type detector. There is, however, an additional complexity compared with alkali-metal atoms due to the electron correlation between the two valence electrons. Therefore whether and how much the spin of the two valence electrons for a bound state can be polarized, and also whether and how much the spin of photoions and photoelectrons remains spin polarized upon breakup (photoionization) of the system is far from obvious: Recall that both photoions and photoelectrons have orbital as well as spin angular momenta, where only the spin angular momenta are to be polarized. Prior to the present work, we have reported the experimental observation of spin-polarized  $Sr^+$  ions using two-color nanosecond laser pulses [9,10], which agrees well with our theoretical prediction [8]. Encouraged by the results with nanosecond lasers, we have further carried out a theoretical investigation of ultrafast spin polarization for alkaline-earth-metal atoms using short laser pulses [11,12], in which we predict that, in spite of the complexity due to the presence of two valence electrons, ultrafast spin polarization of photoions will be possible. Clearly, experimental demonstration of such a scheme would open a new avenue for coherent control of *spin* in atomic and molecular physics.

Related to our work, control of spin has become very popular in semiconductors, quantum wells, and quantum dots in recent years [13–16], and this field is termed “spintronics” [14]. Most of these studies deal with the spin of an electron-hole pair, which is somewhat similar to a bound state in an atomic system and does not involve any breakup processes.

In this paper we demonstrate all-optical control and direct detection of ultrafast spin polarization in a multi-valence-electron system upon breakup of the system through photoionization. Using laser-induced fluorescence (LIF) we can directly and optically detect spin polarization of photoions in an absolute scale [9,10] as a function of time delay between the pump and probe pulses. In contrast, most of the experiments performed with semiconductors, quantum wells, and quantum dots often employ Faraday rotation [13] or magneto-optical Kerr rotation [14] to detect spin, and as a result determination of spin polarization in an absolute scale is rather difficult.

The system we consider is shown in Fig. 1(a), which is essentially the same as the one proposed in Ref. [11], except

\*[t-nakajima@iae.kyoto-u.ac.jp](mailto:t-nakajima@iae.kyoto-u.ac.jp)

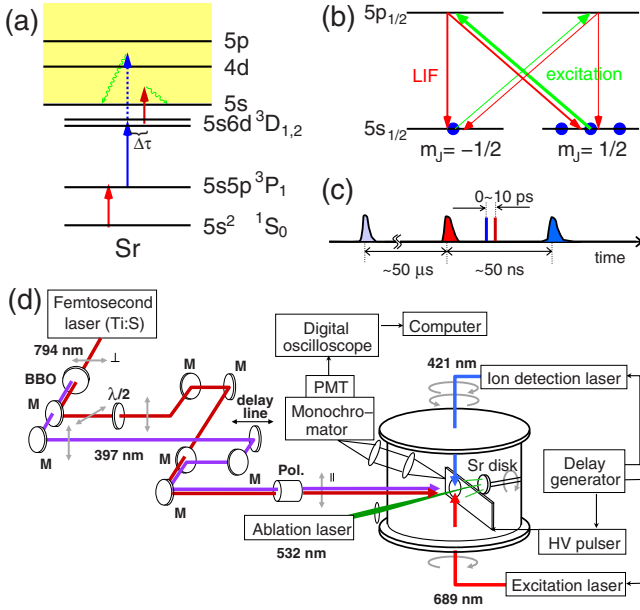


FIG. 1. (Color online) (a) Level scheme, (b) optical detection of spin polarization, and (c) pulse timing for the ablation, excitation, pump, probe, and ion detection laser pulses. (d) Experimental setup.

that different atoms are used in this work due to the available wavelengths of femtosecond laser pulses. The most important ingredient in our scheme is to use a multi-valence-electron atom and introduce a femtosecond pump pulse to produce a coherent superposition of fine structure manifold and ionize the atom by the femtosecond probe pulse after variable time delay. Since we use alkaline-earth-metal atoms, we can directly detect spin polarization of photoions through LIF, as shown in Fig. 1(b), by using the right-(left)-circularly-polarized ion detection laser [9,10]. The time sequence of all laser pulses is shown in Fig. 1(c). The choice of a multi-valence-electron system such as Sr also offers the possibility to simultaneously produce spin-polarized photoions and photoelectrons [8].

The experimental setup is similar to the previous one for the nanosecond laser experiments [9,10], except that we have now introduced a femtosecond laser system. It consists of a vacuum chamber, three nanosecond lasers for ablation, excitation, and ion detection, two femtosecond lasers for the pump and probe, and an optical detection system, as shown in Fig. 1(d). A solid Sr disk on a rotating mount is placed in a vacuum chamber maintained at the pressure of  $\sim 1 \times 10^{-4}$  Pa by two turbomolecular pumps. The second-harmonic pulse of a neodymium-doped yttrium aluminum garnet (Nd:YAG) laser operated at 10 Hz is loosely focused onto the Sr disk with an  $f=25$  cm lens to produce an ablation plume which consists of neutral Sr atoms as well as Sr ions. At 1  $\mu$ s after the ablation pulse, we apply a pulsed electric field of 1 kV with 25  $\mu$ s duration to an ion deflector electrode to prevent ablation ions from flying into the interaction area. We have confirmed that the influence of the residual ions is negligible in the following experiments. About 50  $\mu$ s after the ablation pulse, a right-circularly-polarized excitation pulse (689 nm) with  $\sim 15$  ns duration is turned on to excite  $5s5p^3P_1$  ( $m_j=+1$ ), which serves as an initial state

for the following pump-probe ionization. The linearly polarized pump pulse (397 nm, 150 fs), delivered from the amplified femtosecond laser system (Hurricane, Spectral Physics) with a  $\beta$ -barium borate (BBO) crystal of 0.2 mm thickness, coherently excites the fine structure manifold  $5s6d^3D_1$  and  $^3D_2$ . The time-delayed probe pulse (794 nm, 100 fs) ionizes the atoms in the  $5s6d^3D_1$  and  $^3D_2$  states. After the femtosecond pump-probe pulses we introduce the nanosecond ion detection laser (421 nm) with right- (left)-circular polarization to detect spin-polarized  $\text{Sr}^+ 5s_{1/2}$  ( $m_j = \pm 1/2$ ) ions through the LIF measurement with a time-gated photomultiplier. In order to determine time zero for the delay, we have utilized the third-harmonic of the pump and probe pulses in air by a  $\beta$ -BBO crystal of 0.5 mm thickness through the same glass material with the same thickness used for the optical window of the vacuum chamber so that the third-harmonic intensity becomes maximum. After the loss of optical mirrors, etc., the pulses energies at the interaction zone are estimated to be 80  $\mu$ J, 40  $\mu$ J, 240  $\mu$ J, and 50 nJ, respectively, for the 689, 397, 794, and 421 nm laser pulses with a beam diameter of 4 mm.

There are some complexities in the above experiments to be mentioned: It turns out that the intensity of the pump pulse must be kept rather low to avoid two-photon ionization [dashed arrow in Fig. 1(a)] which contribute more significantly to the LIF signal than the much more intense probe pulse. This kind of puzzling phenomenon would not happen if alkali-metal atoms were used. A careful study of the ionization spectra using tunable nanosecond pulses has shown that there are a few reasons. The most critical one is that the ionization cross section by the probe wavelength is too small compared with that by the pump wavelength. Given the output energy of the fundamental pulse, 900  $\mu$ J, from the regenerative amplifier, 240  $\mu$ J/pulse for the probe pulse is the best we can get. Therefore, we cannot increase the pump pulse energy more than 40  $\mu$ J, which results in the small populations in  $5s6d^3D_1$  and  $^3D_2$ , and accordingly the low ionization yield. Due to the above, stringent optimization of the entire system is required to attain the reasonable but still limited signal-to-noise ratio.

Experimental results are shown in Figs. 2(a)–2(c) as a function of time delay between the pump and probe pulses. Figures 2(a) and 2(b) are the LIF signals by the left-(right)-circularly-polarized ion detection laser, which are proportional to the yields of  $\text{Sr}^+ 5s_{1/2}$  ions with up- (down) spin. It can be seen that  $\text{Sr}^+$  ions with up spin [Fig. 2(a)] have a modulation period of about 6.7 ps, which coincides with the spin-orbit coupling time of  $5s6d^3D_1$  and  $^3D_2$ . This is nothing but a quantum beat. Note, however, that a quantum beat in the spin-resolved signal has never been reported in the literature. As for  $\text{Sr}^+$  ions with down spin [Fig. 2(b)], the modulation is not clear due to the limited signal-to-noise ratio. The variation of spin polarization is plotted in Fig. 2(c) where the spin polarization  $P$  is defined as  $P = (I_{\text{LCP}} - I_{\text{RCP}}) / (I_{\text{LCP}} + I_{\text{RCP}})$  with  $I_{\text{RCP}}$  ( $I_{\text{LCP}}$ ) being the LIF intensity for the right- (left)-circularly-polarized ion detection laser. Clearly, spin polarization is also modulated in time with the period, which also coincides with the spin-orbit coupling time.

For better understanding of the experimental results in

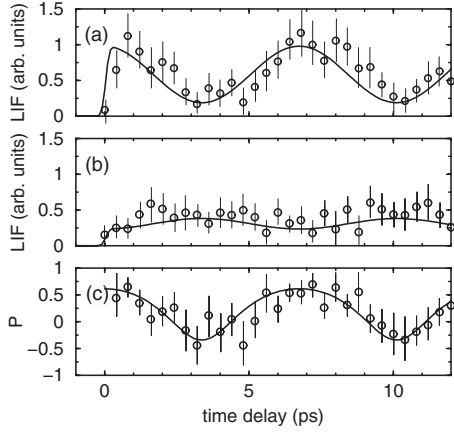


FIG. 2. LIF signals from the (a)  $\text{Sr}^+ 5s_{1/2}(m_j=+1/2)$  and (b)  $\text{Sr}^+ 5s_{1/2}(m_j=-1/2)$  states for the left- (right-)circularly-polarized ion detection laser, and (c) spin polarization as a function of time delay between the pump and probe pulses. *Ab initio* theoretical results are shown by solid lines in each graph.

Fig. 2, we have carried out a theoretical analysis. First, by Hartree-Fock calculations [17], we have checked that both  $5s6d\ ^3D_1$  and  $\ ^3D_2$  states have more than 95% state purity, which enables us to carry out the theoretical analysis we have developed in our previous studies for the weak-field limit [11] and for arbitrary intensities with arbitrary pulse shapes and durations [12]. To provide a clear physical picture, it is more convenient to present the equations for the weak-field limit [11] as summarized below. Briefly, a coherent superposition of  $5s6d\ ^3D_1$  ( $m_j=+1$ ) and  $5s6d\ ^3D_2$  ( $m_j=+1$ ) after the pump pulse can be written as

$$|\Psi(t)\rangle = \frac{-1}{2\sqrt{6}}|5s6d\ ^3D_1\rangle + \frac{\sqrt{3}}{2\sqrt{10}}|5s6d\ ^3D_2\rangle e^{-i\Delta Et}, \quad (1)$$

where the origin of the time  $t$  is chosen to be the instant of the pump pulse, and  $\Delta E$  is the energy difference between  $5s6d\ ^3D_1$  and  $\ ^3D_2$ . After some algebra, populations of photons in each spin state are derived as [11]

$$P_{\uparrow}(t) = \frac{49}{3600} \left( 1 + \frac{33}{49} \cos \Delta Et \right) |R_{5s6d}^{5skp}|^2 + \frac{19}{1400} \left( 1 + \frac{13}{19} \cos \Delta Et \right) |R_{5s6d}^{5skf}|^2, \quad (2)$$

$$P_{\downarrow}(t) = \frac{1}{400} (1 + \cos \Delta Et) |R_{5s6d}^{5skp}|^2 + \frac{1}{100} \left( 1 - \frac{3}{7} \cos \Delta Et \right) |R_{5s6d}^{5skf}|^2, \quad (3)$$

where  $R_{5s6d}^{5sep}$  and  $R_{5s6d}^{5sef}$  are the bound-free radial matrix elements from  $5s6d$  to the  $5sep$  and  $5sef$  continua, respectively. Note that the small fine structure interval,  $4.95\text{ cm}^{-1}$ , between  $\ ^3D_1$  and  $\ ^3D_2$  allows us to assume that the radial wave functions of those states are nearly the same. Now all the two-electron states are constructed by using the model potential [18] and the configuration interaction approach by

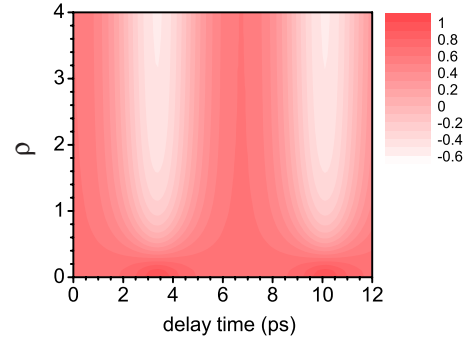


FIG. 3. (Color online) Spin polarization as a function of time delay between the pump and probe pulses and the ratio of the bound-free matrix elements,  $\rho$ .

expanding the wave functions in the discretized  $B$ -spline basis set [19], from which we have calculated the bound-free radial matrix elements  $R_{5s6d}^{5sep}$  and  $R_{5s6d}^{5sef}$  for our probe laser wavelength, and obtained them to be 2.63 and 3.37 a.u., respectively. Although the use of Eqs. (1)–(3) is convenient to understand the essence of the physics, these equations cannot account for the finite pulse duration. Therefore, for comparison with the experimental data we have employed the more general formalism [12] instead of Eqs. (1)–(3). The *ab initio* theoretical results are shown in Figs. 2(a)–2(c) by

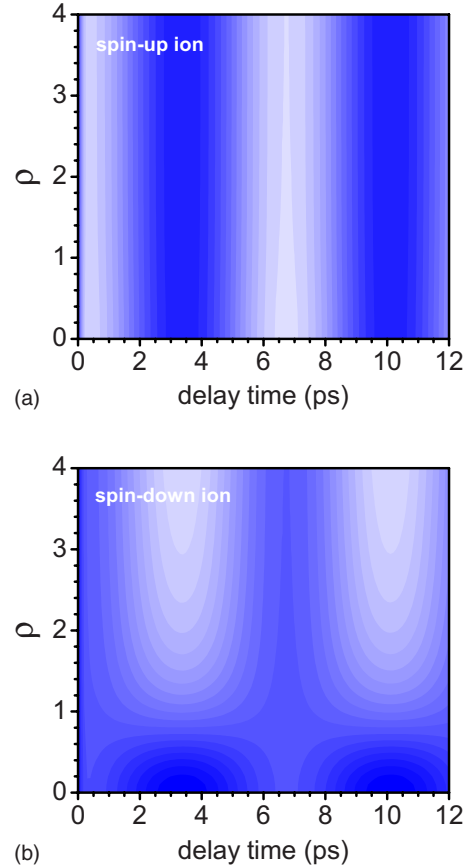


FIG. 4. (Color online) Yield of (a) spin-up and (b) spin-down ions as a function of time delay between the pump and probe pulses and the ratio of the bound-free matrix elements,  $\rho$ .

the solid lines. The agreement is reasonably good. Note that the effect of the finite pulse duration is clearly seen around time zero.

From Eqs. (1)–(3), it is clear that the behavior of the spin polarization critically depends on the ratio  $\rho \equiv R_{5s6d}^{5sep} / R_{5s6d}^{5sef}$ , which will vary with the probe laser wavelength. To obtain some insight, we have performed further calculations by changing the value of  $\rho$ . The results are shown in Figs. 3 and 4, respectively. As we can clearly see in Fig. 3, the minimum value of spin polarization even becomes negative if  $\rho > 0.8$ . It is very interesting to note that, if  $\rho < 0.7$ , the modulations of the yields of spin-up (-down) ions, shown in Figs. 4(a) and 4(b), are in phase, while for  $\rho > 0.7$ , they are antiphase due to the peculiar behavior of the yield of spin-down photoions, whose origin can be traced back to Eq. (3). These results clearly show that the dynamics of spin polarization would be significantly different for different probe laser wavelengths.

In conclusion, we have experimentally demonstrated all-optical control and direct detection of ultrafast spin polarization of photoions upon breakup of a multi-valence-electron

system. Due to the presence of electron correlation, how much spin polarization takes place in photoions and photoelectrons upon breakup is far from obvious, in contrast to the case of a single-valence-electron system. Nevertheless, we have successfully controlled and measured the degree of ultrafast spin polarization in an absolute scale using a pump-probe technique. We have also performed *ab initio* theoretical calculations and compared the results with the experimental data. The agreement turned out to be reasonably good. Our results could open a new avenue for coherent control of spin in atomic and molecular physics. The advantage of using a multi-valence-electron system is that not only photoions but also photoelectrons will presumably be spin polarized [8,11]. In this respect, simultaneous measurement of spin polarization for both photoions and photoelectrons might be interesting for future study.

This work was supported by a Grant-in-Aid for scientific research from the Ministry of Education and Science of Japan.

- 
- [1] R. S. Judson and H. Rabitz, *Phys. Rev. Lett.* **68**, 1500 (1992).  
 [2] T. Brixner, N. H. Damrauer, and G. Gerber, *Adv. At., Mol., Opt. Phys.* **46**, 1 (2001).  
 [3] D. J. Tannor and S. A. Rice, *J. Chem. Phys.* **83**, 5013 (1985).  
 [4] N. Dudovich, B. Dayan, S. M. Gallagher Faeder, and Y. Silberberg, *Phys. Rev. Lett.* **86**, 47 (2001).  
 [5] R. Netz, A. Nazarkin, and R. Sauerbrey, *Phys. Rev. Lett.* **90**, 063001 (2003).  
 [6] E. Sokell, S. Zamith, M. A. Bouchene, and B. Girard, *J. Phys. B* **33**, 2005 (2000).  
 [7] M. A. Bouchene, S. Zamith, and B. Girard, *J. Phys. B* **34**, 1497 (2001).  
 [8] T. Nakajima and N. Yonekura, *J. Chem. Phys.* **117**, 2112 (2002).  
 [9] T. Nakajima, N. Yonekura, Y. Matsuo, T. Kobayashi, and Y. Fukuyama, *Appl. Phys. Lett.* **83**, 2103 (2003).  
 [10] N. Yonekura, T. Nakajima, Y. Matsuo, T. Kobayashi, and Y. Fukuyama, *J. Chem. Phys.* **120**, 1806 (2004).  
 [11] T. Nakajima, *Appl. Phys. Lett.* **84**, 3786 (2004).  
 [12] T. Nakajima, *Appl. Phys. Lett.* **88**, 111105 (2006).  
 [13] N. H. Bonadeo, J. Erland, D. Gammom, D. Park, D. S. Katzer, and D. G. Steel, *Science* **282**, 1473 (1998).  
 [14] S. A. Wolf, D. D. Awschalom, R. A. Buhrman, J. M. Daughton, S. von Molnár, M. L. Roukes, A. Y. Chtchelkanova, and D. M. Treger, *Science* **294**, 1488 (2001).  
 [15] J. A. Gupta, R. Knobel, N. Samarth, and D. D. Awschalom, *Science* **292**, 2458 (2001).  
 [16] R. D. R. Bhat and J. E. Sipe, *Phys. Rev. Lett.* **85**, 5432 (2000).  
 [17] R. D. Cowan, *The Theory of Atomic Structure and Spectra* (University of California Press, Berkeley, 1981).  
 [18] C. H. Greene and M. Aymar, *Phys. Rev. A* **44**, 1773 (1991).  
 [19] T. N. Chang and X. Tang, *Phys. Rev. A* **44**, 232 (1991).